Bull Volcanol (2009) 71:559–574
DOI 10.1007/s00445-008-0242-x

RESEARCH ARTICLE

Landslide and tsunami hazard at Yate volcano, Chile as an example of edifice destruction on strike-slip fault zones

Sebastian F. L. Watt · David M. Pyle · José A. Naranjo · Tamsin A. Mather

Received: 8 February 2008 / Accepted: 15 August 2008 / Published online: 18 September 2008

Abstract The edifice of Yate volcano, a dissected stratocone in the Andean Southern Volcanic Zone, has experienced multiple summit collapses throughout postglacial time restricted to sectors NE and SW of the summit. The largest such historic event occurred on 19th February 1965 when ~6.1–10×10^6 m^3 of rock and ice detached from 2,000-m elevation to the SW of the summit and transformed into a debris flow. In the upper part of the flow path, velocities are estimated to have reached 40 m s^{-1}. After travelling 7,500 m and descending 1,490 m, the flow entered an intermontane lake, Lago Cabrera. A wavemaker of estimated volume 9±3×10^6 m^3 generated a tsunami with an estimated amplitude of 25 m and a run-up of ~60 m at the west end of the lake where a settlement disappeared with the loss of 27 lives. The landslide followed 15 days of unusually heavy summer rain, which may have caused failure by increasing pore water pressure in rock mechanically weathered through glacial action. The preferential collapse directions at Yate result from the volcano's construction on the dextral strike-slip Liquiñe-Ofqui fault zone. Movement on the fault during the lifetime of the volcano is thought to have generated internal instabilities in the observed failure orientations, at ~10° to the fault zone in the Riedel shear direction. This mechanically weakened rock may have led to preferentially orientated glacial valleys, generating a feedback mechanism with collapse followed by rapid glacial erosion, accelerating the rate of incision into the edifice through repeated landslides. Debris flows with magnitudes similar to the 1965 event are likely to recur at Yate, with repeat times of the order of 10^2 years. With a warming climate, increased glacial meltwater due to snowline retreat and increasing rain, at the expense of snow, may accelerate rates of edifice collapse, with implications for landslide hazard and risk at glaciated volcanoes, in particular those in strike-slip tectonic settings where orientated structural instabilities may exist.

Keywords Volcanic landslide · Debris flow · Yate volcano · Edifice collapse · Liquiñe-Ofqui fault zone · Tsunami · Strike-slip

Editorial responsibility: J. Stix

S. F. L. Watt (✉) · D. M. Pyle · T. A. Mather
Department of Earth Sciences, University of Oxford,
Parks Road,
Oxford OX1 3PR, UK
e-mail: Sebastian.Watt@earth.ox.ac.uk

J. A. Naranjo
Servicio Nacional de Geología y Minería,
Av. Santa María,
0104 Santiago, Chile

Introduction

A major hazard posed by many volcanoes is that of edifice collapse, generating landslides and associated phenomena on a range of magnitudes and timescales. Such events have been documented at several Pleistocene–Holocene Chilean volcanoes (Sepúlveda et al. 2006), the dominant cause usually being massive slope failure unrelated to volcanic activity rather than explosive edifice destruction (e.g. Siebert 1984). External triggers implicated in non-volcanogenic collapses include earthquakes (e.g. Davis and Karzulovíc 1963; Scott et al. 2001) and extreme rainfall (Iverson 2000), commonly acting on rocks previously weakened through hydrothermal alteration. In this paper, we document recent examples of partial edifice collapse at a volcano in the southern Andes of Chile. We show how events may have

been conditioned by the tectonic setting—the close spatial association with an active strike-slip fault system—and we place these events in the context of the continuing post-glacial evolution of volcanic edifices in southern Chile.

Yate volcano

Yate is a compound volcano situated at 41.8° S in the Andean Southern Volcanic Zone on the Hualaihué peninsula, Chile (Fig. 1). The north–south trending Yate complex comprises bedded Pleistocene lavas and pyroclastic rocks overlying a Plio-Pleistocene volcanic basement. Together with the west–east trending Cordillera Pululil/Candelaria ridges (Fig. 1), this forms a cruciform edifice with a basal diameter of 20 km. The structure is glacially eroded, but has grown through Holocene effusive activity. Although there are no records of historical volcanic activity at Yate, we have found tephrochronological evidence for minor postglacial explosive eruptions. The edifice lies on the regional dextral strike-slip Liquiñe-Ofqui fault zone (LOFZ) which extends for over 1,000 km along the volcanic arc of southern Chile (Cembrano et al. 1996; Fig. 1).

South of Yate, a glacially sculpted valley marks the course of the LOFZ (cf. Cembrano et al. 1996). Within this valley, the Holocene volcano Hornopirén forms an elliptical cone, blocking drainage southwest of Yate to form the Lago Cabrera basin. A lake is likely to have formed here following early Holocene eruptions of Hornopirén, with subsequent eruptions producing a narrower and deeper basin. The present-day lake has an area of approximately 5 km^2 (Fig. 2).

Deglaciation proceeded rapidly at these latitudes at the end of the last glaciation and was nearly complete by 12,300 ^{14}C yr BP (Heusser 2002). The summit ridge of Yate still supports glaciers, with a snowline at ~1,500 m. Aerial photographs indicate significant snowline retreat in recent decades, a feature that has been widely recognised in the southern Chilean Andes (Carrasco et al. 2005).

Past landslides at Yate

Destruction of Yate's summit by successive collapses probably began soon after the end of the last glaciation. Debris flows, originating from rockfalls high on the flanks of Yate, have formed fan deposits at the east end of Lago Cabrera, SSW of the summit, and at Llanos del Yate to the

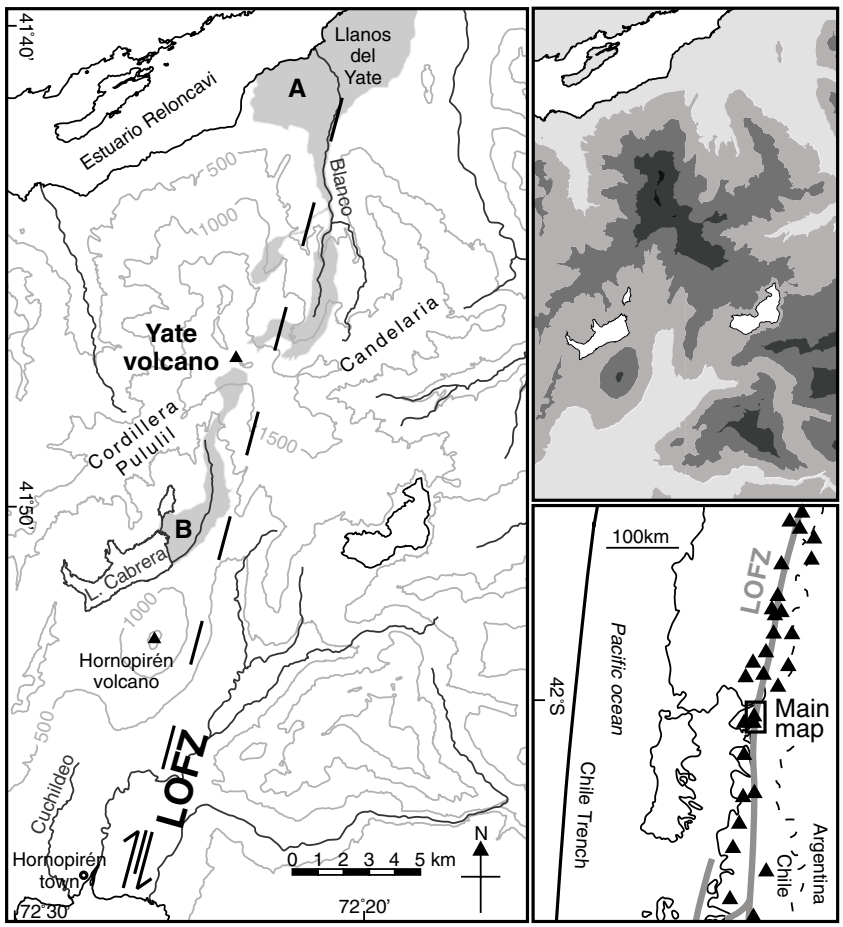

Fig. 1 *Main panel*: Topography of Yate volcano and the surrounding area, showing the approximate line of the Liquiñe-Ofqui fault zone (*LOFZ*), on which the volcanoes Yate and Hornopirén lie. Also shown are the extent of damage and deposition caused by debris flows from the NNE and SSW summit areas in **A** 1870 and 1896 (Hauser 1985) and **B** 1965 and 2001. *Upper right*: Shaded relief map of the area in the main panel, from sea level (*white*) to >2,000 m (*black*) at 500-m intervals. *Lower right*: A map showing the central portion of the Andean Southern Volcanic Zone, marking the LOFZ and volcano locations

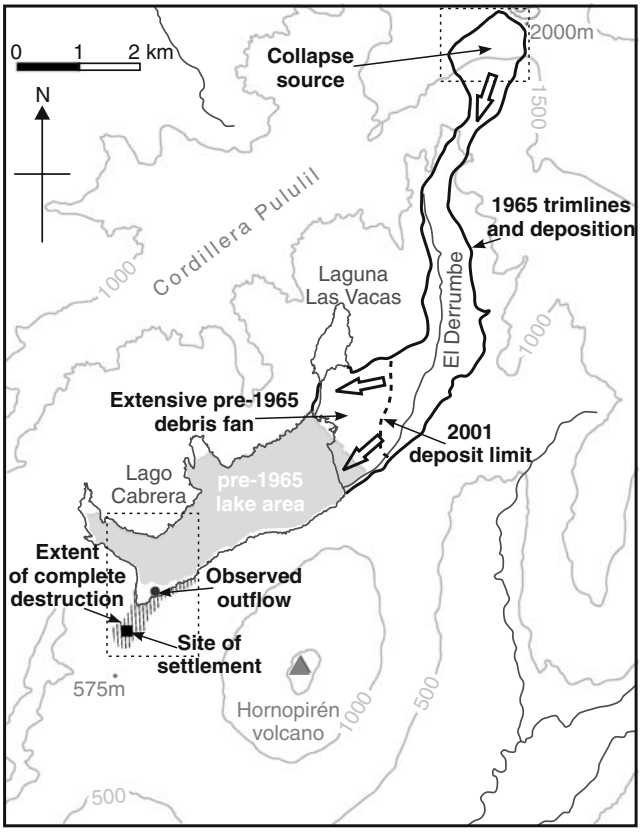

Fig. 2 Map of the SW sector of Yate volcano and Lago Cabrera showing the extent of major historic debris flows, the change in shoreline of Lago Cabrera following the 1965 landslide, debris flow and tsunami and the principal area of destruction due to the tsunami. *Dashed boxes* show the position of the aerial photo detail in Figs. 4c and 6

NNE (Fig. 1), extensively modifying local topography. Landslides originate from horseshoe-shaped collapse scars NE and SW of Yate's summit area. The resultant mass movements are modified and controlled by local topography and consist of volcanic rock and ice; they are best classified as volcanic debris flows. Historical records suggest that most of the fan material was emplaced during large individual events, four of which have occurred since 1870 (Flash 1965; Hauser 1985; El Mercurio 2001).

Major collapses NNE of Yate occurred in 1870 and 1896 (Fig. 1; Hauser 1985), with debris following the Rio Blanco to the coast at Llanos del Yate. Here, deposits from the two events cover an area of ~25 km^2 and blanket a region of gentle topography. The extent of the fan at Llanos del Yate and the scale of the collapse scars at Yate's summit suggest that such landslides have been frequent throughout post-glacial time. Debris flows occurred SSW of Yate in 1965 and 2001. The deposits are confined to the Lago Cabrera area (Fig. 2) and form the hummocky outflow of the El Derrumbe valley. This name, meaning landslide, was given to the valley prior to 1965 and suggests local awareness of the instability of Yate's summit. The El Derrumbe debris fan has built westward and upward over time, modifying and raising the lake shoreline. Here, we examine in detail the largest recorded landslide from Yate's SW sector, which occured in 1965. We investigate the immediate and long-term factors that give rise to repetitive mass-wasting events at Yate in an effort to estimate the frequency and characterise the scale of this type of event. In particular, we focus on the role of glacial erosion and deglaciation and show how the pattern of edifice collapse is consistent with a model of volcano deformation by the underlying strike-slip LOFZ.

The 1965 Yate landslide and Lago Cabrera tsunami

The most catastrophic historic landslide at Yate occurred in 1965 when a mass of rock and ice detached from SW of Yate's summit. The failed material was transported south down the confined El Derrumbe valley, and its runout and super-elevation behaviour is consistent with rapid transformation into a saturated debris flow, which incorporated debris from below the collapse scar and entrained vegetation along its path. Unfortunately, its remoteness and inaccessibility due to dense forest meant that close examination of the deposit was not possible, limiting our interpretations of the failed rock body and the proportions of entrained material. Whilst the flow regime cannot be directly ascertained, comparison may be made with debris flow deposits NE of Yate. Here, the two historic events formed saturated debris flows with long run-outs, altering the course of the Rio Blanco on the Llanos del Yate debris fan (Hauser 1985). The deposits are poorly sorted mixtures of rock, ash, sand, soil and vegetation, but lack fine material and mud, with clasts of up to 7-m diameter (Hauser 1985). Deposits SW of Yate contain boulders of up to 2-m diameter and form mounds and hollows on length scales of ~10–30 m, although some of this relief may be inherited from older debris fan deposits. The scale of these features is similar to the deposits NE of Yate. Hollows within the deposit suggest that large ice blocks were present, analogous to the 'kettles' observed by Hauser (1985) at the Llanos del Yate and described from many rock and ice collapse deposits (e.g. Branney and Gilbert 1995; Clavero et al. 2002). Thus, morphological evidence, from photographs and from field examination using binoculars, suggests that deposits SW of Yate are comparable to those produced by the saturated debris flows NE of the summit, which originated from landslides in the same lithologies and travelled similar courses.

Part of the debris flow entered Lago Cabrera, generating an impulse wave, the effects of which are still clearly visible around the lakeshore. Here, we use field observations, eyewitness interviews and aerial images from 1960

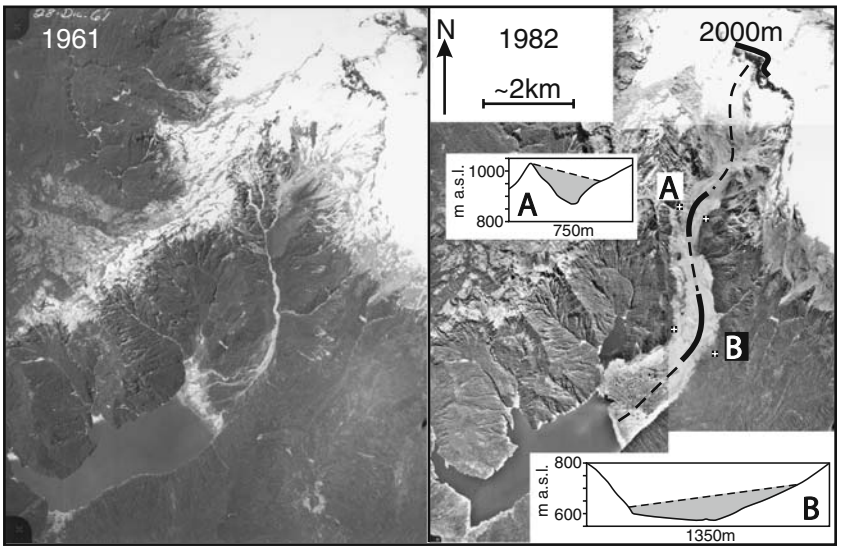

Fig. 3 Aerial photographs of the 1965 landslide and debris flow region SW of Yate taken in 1961 and 1982. Locations of the bends in the path used for flow velocity calculations and the centreline of the flow are shown on the 1982 photograph. *Inset*: topographic cross-sections (vertical scale exaggerated) show the height of vegetation trimlines used to estimate super-elevation

and 1982 to analyse this event. The smaller 2001 debris flow followed a similar course, partially covering the 1965 deposits. There is no evidence to suggest that it reached Lago Cabrera, though it killed 50 cattle in the lower El Derrumbe valley (El Mercurio 2001). The unvegetated 2001 deposit covers about one third of the 1965 subaerial deposit, primarily on the south side of the lower El Derrumbe valley. The 2001 flow left fresh vegetation trimlines in the upper El Derrumbe, but due to the lack of aerial photography following this event, we are unable to locate the source or quantify the scale of this event. Ground-based observations and 1982 aerial photographs suggest that the 2001 debris flow did not originate from the same part of the summit region as the 1965 landslide.

Accounts and observations

In the early morning of 19th February 1965, a landslide resulting from a collapse SW of Yate's summit produced a debris flow that travelled down the El Derrumbe valley and entered the northeast end of Lago Cabrera (Fig. 2). Farm buildings, sited on the fan at this end of the lake, were buried without trace. The debris flow overran older vegetated deposits and entered the lake, extending the pre-event shoreline westward by up to 250 m. The surface of the 1965 flow deposit is uneven and variably vegetated, and its upper part is now buried under the 2001 deposit.

An impulse wave, generated as the debris flow entered the water, travelled the length of Lago Cabrera, running up over gently sloping land bordering the southwest corner of Lago Cabrera (Figs. 2 and 3). Here, three farmhouses were destroyed, and 27 inhabitants were killed (Flash 1965). Eyewitness accounts (Appendix 1) record just one wave, synchronous with the first noise, possibly followed by a second loud sound. Land along the lake shorelines, and particularly in the populated southwest corner, was scoured of vegetation, including mature coigüe forest, up to 35–40 m above the present shoreline (Fig. 4a–c). The debris entering the lake included rock, snow and ice, but the damage around the lake was caused entirely by the water wave, which deposited only 20–30 cm of fine mud at the west end where it ran inland. This deposit is preserved below felled tree trunks and contains intraclasts (Fig. 4d), with rare angular lithic fragments that increase in frequency and size (up to a few centimetre in diameter) towards the shoreline.

The Lago Cabrera shoreline was altered by the 1965 landslide (Fig. 2). An eyewitness estimated an increase in water level of 6 m immediately following the event, but aerial photograph analysis suggests a change of 10–15 m. The deposit blocked drainage at the northeast end of the lake, forming Laguna Las Vacas, with surface area 0.45 km^2 (CONAF 2007). A drowned forest is still evident at the shallow north end of this lake.

Analysis of the 1965 debris flow and tsunami

We have estimated the scale of the 1965 events from aerial photographs, maps and field measurements and have attempted to quantify the scale of the subsequent tsunami in Lago Cabrera, primarily to assess the approximate wavemaker volume (i.e. the volume of the submerged deposit). Estimates of lake bathymetry and the extent of the submerged deposit are poorly constrained, and the sensitivity of results to these uncertainties are discussed in the following sections. Results should be regarded as semi-quantitative, but are made in an effort to constrain the parameters relevant to the 1965 landslide.

Four regions relating to the landslide and tsunami are defined for the following section (Fig. 5): the collapse

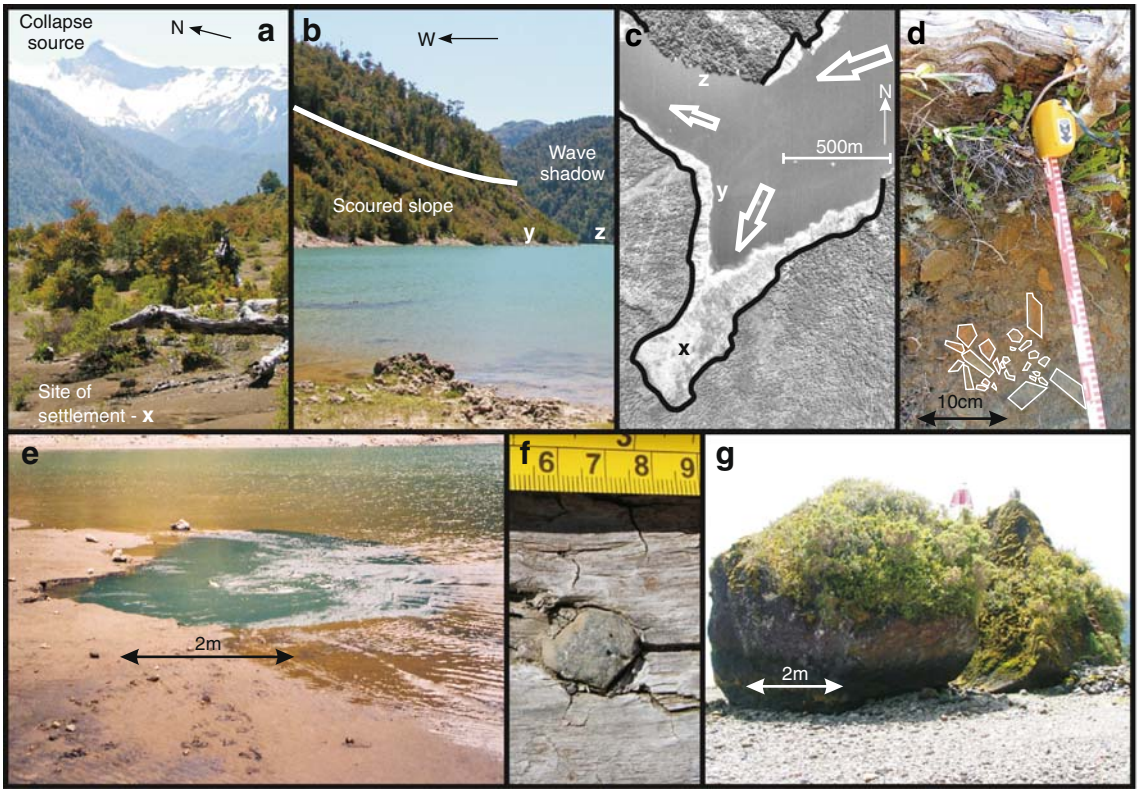

Fig. 4 Photographs of Lago Cabrera showing effects of the tsunami following the 1965 landslide. **a** SW corner of lake, showing bare ground and young vegetation in zone of complete stripping of cover, and the approximate site of the settlement, several hundred metres from the lake shore. The summit area of Yate is in the background. **b** SW corner of lake showing vegetation scour up to 30 m above present water level. On the west-facing opposite bank, in the shadow of the eastward travelling wave, large trees extend to the lake shore. **c** Aerial photograph of SW corner of Lago Cabrera following the 1965 tsunami showing directions of wave motion. Points *x y z* refer to locations shown in images **a** and **b**. **d** Intraclasts of rip-up soil fragments in the mud deposit left at the SW corner of Lago Cabrera following the tsunami preserved under a felled tree. Selected clasts have been *outlined* for clarity. **e** Lago Cabrera outflow at the edge of muds at the SW lakeshore carrying water beneath Hornopirén lavas. **f** Embedded clast in wood of felled trunk at SW corner of lake; scale in centimetres. **g** Individual fractured clast of volcanic rock from the NE summit of Yate carried in the debris flow of 1870 or 1896 and transported approximately 12 km from source

source, the upper El Derrumbe valley, the lower El Derrumbe valley and debris fan, and the submerged deposit and Lago Cabrera.

The collapse source

Aerial photographs from 1961 show debris trails on the upper slopes of Yate, indicating active erosion of steep slopes below the crags (Fig. 6). Similar features are seen on the 1982 images, and at the present day the snow below the higher cliff faces is littered with fallen rock.

Detailed examination of aerial photographs bracketing the 1965 landslide indicates a collapse source near the summit ridge of Yate (Fig. 6) in a southward-opening amphitheatre-shaped depression. This feature is likely to be the result of previous collapses, coupled to some degree with subsequent glacial erosion. Collapse occurred in two main areas, one on each side of this depression, across a maximum E–W width of 1.3 km. All of the material removed in the collapse entered the El Derrumbe valley through a narrow (~400 m) opening at the head of the valley.

A deep-seated landslide, generated on the east side of the depression, left a subvertical cliff, with a headscarp breadth of 700 m. The shape and scale of this cliff face has been reconstructed by ground-based photogrammetry (PicWorks, R. Herd, personal communication) using two images taken from the lakeshore, approximately 10 km from the summit area, with a line-of-sight angle of 10°. Using five georeferenced control points, *xyz* coordinates were calculated for over 700 matched points on each image to create a 3D surface model of the cliff morphology (Fig. 7). The photographs and model reveal a subvertical upper cliff face, formed of subhorizontal lavas, up to 80 m thick. The lavas overlie a lower cliff of heavily weathered rocks, judged from their appearance to be pyroclastic material, up to 100 m thick, with more uneven topography. The pyroclastic rocks erode recessively as a series of gullies with a concave profile, becoming snow-covered and ending in a small

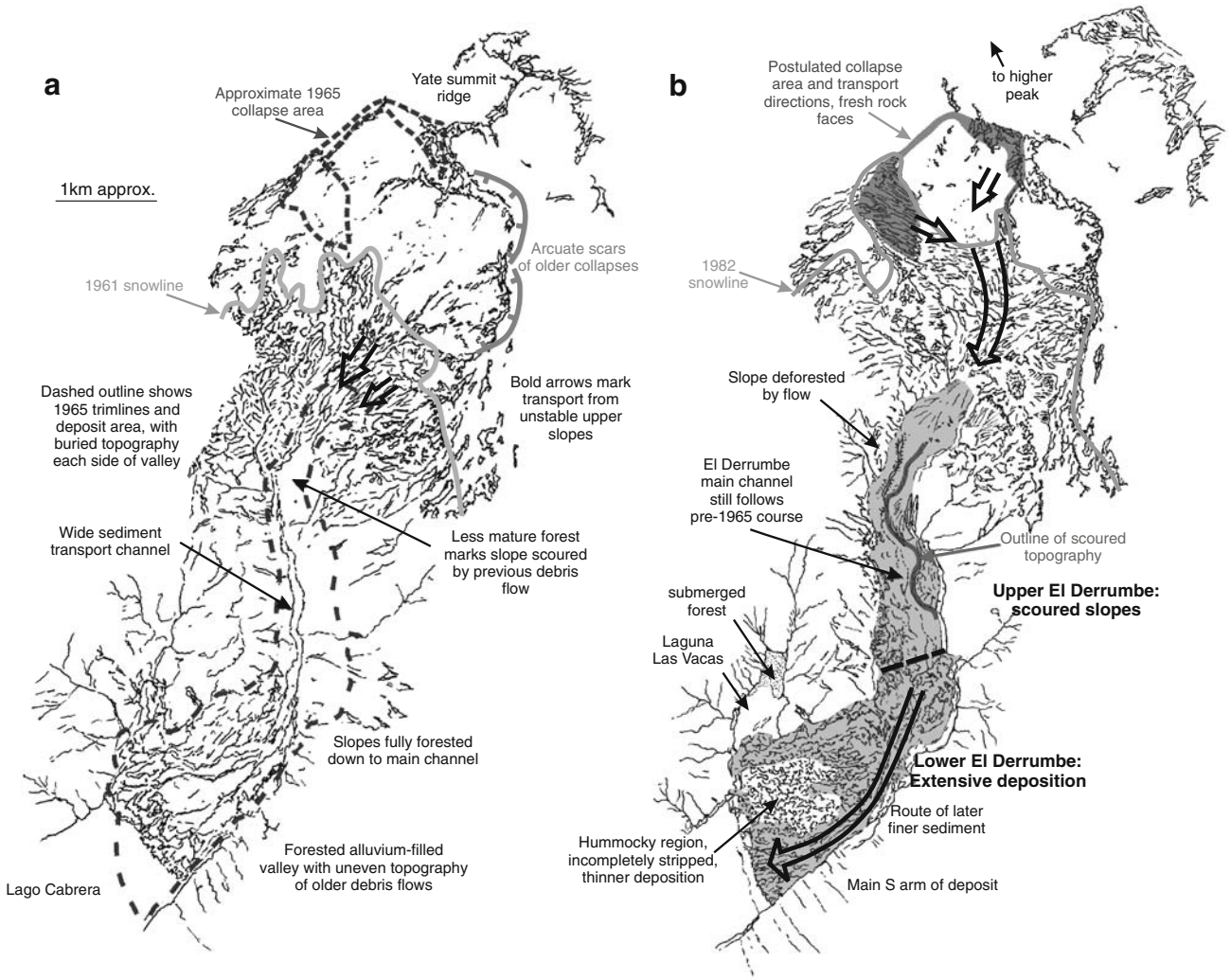

Fig. 5 Aerial photograph interpretations of the area between the summit ridge of Yate and the east end of Lago Cabrera showing features relating to the landslide and debris flow. **a** From photographs taken on 28 December 1961. **b** From photographs taken in 1982. Scale is approximate

plateau at the base. The collapsing mass of rock and ice travelled around the west side of a rocky slope below the plateau, which was exposed after the event and may have been a source of additional debris. According to eyewitness reports, prior to the 1965 landslide, the failure region formed a craggy slope (Fig. 6) with a rounded profile, in contrast to the present-day cliff. It is possible that differential erosion of the pyroclastic rocks underlying the lava cap in the failure region contributed to rock face instability. We suggest that the result was a slump-like valley-head landslide and that similar landslides are likely to recur from the newly exposed cliff.

After the 1965 landslide, 0.1 km^2 of steep stony ground was exposed on the west side of the amphitheatre, in an area that previously had thick ice cover. This shallow slab failure may have occurred simultaneously with the failure on the east side, or in response to it, following entrainment of material at the base of the slope, potentially reducing relative glacier strength here (cf. Huggel et al. 2007). This region contributed a high proportion of ice as well as rock to the landslide.

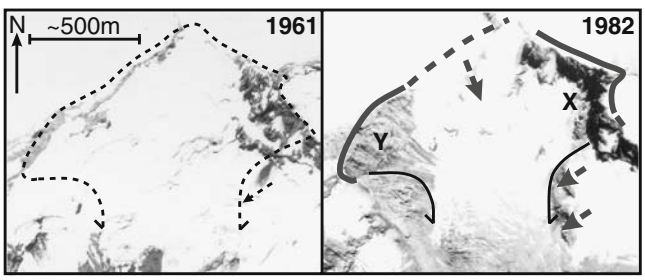

Fig. 6 Aerial photographs of the Yate summit collapse area in 1961 and 1982 showing the main east (*X*) and west (*Y*) source regions of the 1965 landslide

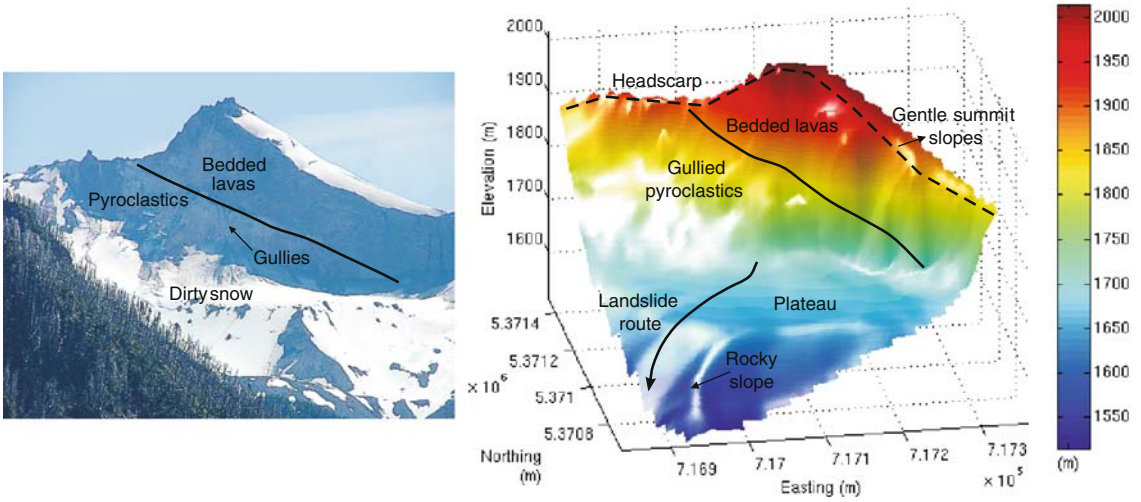

Fig. 7 Photograph and photogrammetric reconstruction of the eastern source of the 1965 landslide. This region contributed the bulk of rocky material to the debris flow and left a cliff of bedded lavas overlying recessively eroding pyroclastic rocks

To estimate the volume of failed material, we treat the collapse source as two main regions. In the east (X in Fig. 6), along a headscarp of 700 m, the mean vertical cliff height is ~150 m. Maps, aerial photographs and eyewitness accounts suggest that the pre-failure slope angle was ~40–50°, implying a rock failure volume of ~$6–9\times10^6$ m^3. To the west (Y in Fig. 6), we estimate that 1–10 m of ice and rock cover was removed from an area of ~0.1 km^2, a volume of 10^5–10^6 m^3. The total source region failure volume was therefore ~6×10^6–1×10^7 m^3, the bulk of which originated from the east cliff. Entrainment of unconsolidated material from the slopes below the failure area is unconstrained, but may have increased this volume substantially (see "Deposit volume").

El Derrumbe valley and debris deposit

A topographic profile of the debris path from the top of the failure scarp at 2,000 m shows a horizontal length of 7,500 m to the pre-event shoreline of Lago Cabrera, with a 1,490-m vertical drop (Fig. 8). Below the collapsed amphitheatre, the slope steepens, marking the top of the El Derrumbe valley.

The most prominent difference between the aerial photographs of 1961 and 1982 is the unvegetated deposit along the El Derrumbe valley (Fig. 3). Prior to the 1965 landslide, the slopes of the upper El Derrumbe were heavily forested. The debris flow cleared vegetation across a 1,100-m width in the north–south trending upper El Derrumbe valley, overriding topography to ~100 m above the valley floor. The river course in the upper El Derrumbe was unaltered by the landslide, and local topographic shapes are still discernible, albeit stripped of vegetation, suggesting only minor deposition in this region.

The lower El Derrumbe valley trends southwest and prior to 1965 had a gently sloping but uneven topography covered by mature forest. The 1965 debris flow overran this area, forming a fan with a maximum width of 1.5 km towards the east lake shore. Although all of the mature forest in this region was cleared by the 1965 debris, the main flow split into two arms, carrying the bulk of material around hummocky topography in the centre of the pre-1965 fan, suggesting deceleration of the flow. In this central area, scrub rapidly reestablished, today forming patches of low woodland close to the lakeshore. In contrast, the clastic material in the main channels has only a sparse cover (Fig. 9). The north arm of debris followed the pre-1965 main river course, damming drainage from the north and forming Laguna Las Vacas. The south arm transported the greater volume of debris, forming a fan at the east end of Lago Cabrera and generating an impulse wave. The modern river follows the south edge of this fan, directly below steep valley slopes. It may have modified the fan morphology through deposition and transport of fine sediment from higher in the valley in the years following the landslide.

Deposit volume

Debris flow deposition in the upper El Derrumbe valley (2.0 km^2; Fig. 5) is considered to be negligible. The debris flow deposited subaerially in the lower El Derrumbe valley (3.0 km^2) where topography suggests an irregular deposit thickness. This reaches thicknesses of ~10 m in some areas, such as the area of blocked drainage that subsequently formed Laguna Las Vacas. From this, we estimate the mean deposit thickness in the lower El Derrumbe valley to be between 3 and 5 m (a volume of 9×10^6–1.5×10^7 m^3) and after accounting for the submerged deposit ("Lago Cabrera

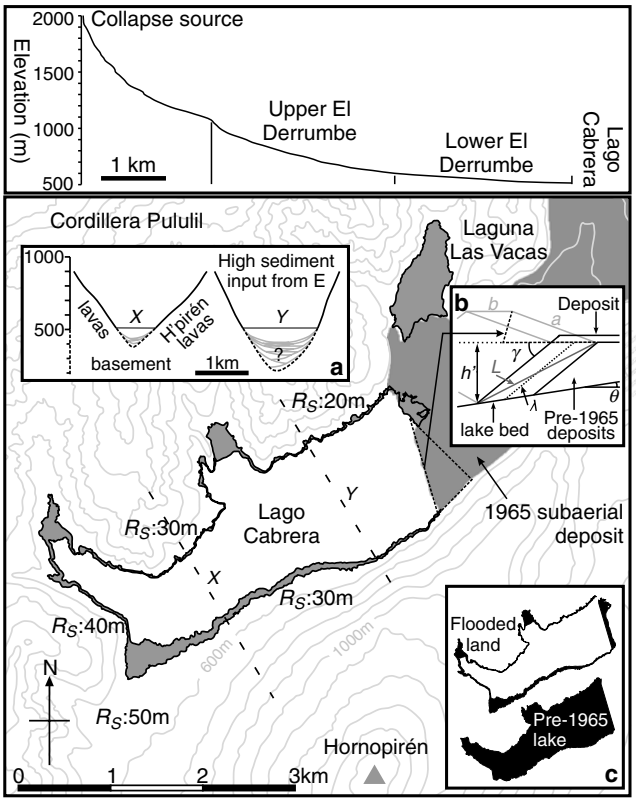

Fig. 8 *Upper*: longitudinal profile of the debris flow route, from the source to the shore of Lago Cabrera (Fig. 3), with divisions into the regions mentioned in the text. *Lower*: map detail of Lago Cabrera after 1965 landslide, with the debris flow deposit *outlined*. Flooded land around the original lake shore is shaded. R_S values show estimates of run-up (above pre-event water level) based on vegetation trimlines. *Insets* show parameters used in calculations in the text. **a** Topographic profiles for two sections across the lake used for bathymetric approximation. **b** Wavemaker dimensions. *Dashed triangle* indicates debris fan extent at the pre-event lake water level. **c** Original and flooded lake areas used to estimate water displacement and lake volume change

and the 1965 tsunami"), a total deposit volume of ~1.5–2.7×10^7 m^3. The collapsed source material would have expanded during disintegration and transformation into a debris flow. Without field constraints, we assume a bulking factor of 0.25, following Hungr and Evans' (2004) use of the median porosity of loosely crushed rock, to infer a pre-bulking source volume of $1.2–2.2\times10^7$ m^3. This is approximately twice as large as the estimated volume of the failure region ("The collapse source"), implying substantial entrainment of colluvium and vegetation along the flow path. The deposit volume is an order of magnitude smaller than some non-eruptive volcanic collapses such as that at Iriga, Philippines (cf. Lagmay et al. 2000) or the 1970 rock and ice avalanche of Nevados Huascarán, Peru. In the debris flow classification scheme (range 1–10) of Jakob (2005), the 1965 event at Yate has a magnitude of ~7. However, the scale and inferred recurrence rate (see "Previous landslides at Yate") of the 1965 and similar-sized events at Yate is high compared to catastrophic flank failures at many volcanoes, such as those at Casita in 1998 (1.6×10^6 m^3; Kerle 2002) and earlier in the Holocene (Scott et al. 2005; see "Previous landslides at Yate").

Velocity estimates

The entire landslide volume was funnelled through a notch ~400 m wide at the head of the El Derrumbe valley, and the flow remained confined for ~5 km before fanning out and decelerating in the lower El Derrumbe valley. Following Evans et al. (1989), the longitudinal horizontal path of 7,500 m and vertical change of 1,490 m give a *fahrböschung* (the ratio of vertical change to horizontal path) of 0.2 (11.3°). This low value indicates a highly mobile flow, and the true value would be significantly lower had the debris not entered Lago Cabrera. Rapid transformation into a debris flow would have been enhanced by entrainment of saturated colluvium (Hungr and Evans 2004). Comparison with similar channelised landslides that developed into debris flows (Evans et al. 1989; Boultbee et al. 2006) suggests that the flow was of high mobility given its volume.

Indirect estimates of debris flow velocity, v, may be derived from evidence of debris flow super-elevation using the vegetation trimline at bends in the flow path (Pierson 1985). From the tilting of the free surface in a bend,

$$v = \sqrt{\frac{gyr}{j}} \quad (1)$$

where g is acceleration due to gravity, y is the difference in trimline elevation, r is the radius of curvature at the centre of the flow path, and j is the channel width. Calculations at two points in the flow path (A and B; Table 1; Fig. 3), using aerial photographs and topographic maps, gave velocities of 27 and 39 m s^{-1}. The application of Eq. 1 has not been rigorously tested for debris flows of this type, and it may underestimate the true velocity (Pierson 1985; Evans et al.

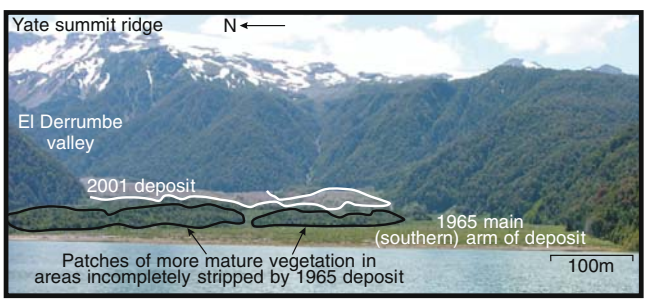

Fig. 9 Photograph looking E towards El Derrumbe debris fan showing features left by the 1965 and 2001 debris flows

Table 1 Debris flow velocity estimates

Location[a]	A	B
y (m)	65	90
r (m)	450	1,750
j (m)	400	1,000
v (super-elevation[b], m s^{-1})	26.8	39.3
v (velocity head[b], m s^{-1})	35.7	42.0

[a] See Fig. 3
[b] Pierson (1985)

2001). Using a velocity-head calculation at the same points (Pierson 1985; Table 1), based on the conversion of kinetic to gravitational potential energy, gives comparable but slightly higher velocities:

$$v = \sqrt{2gy} \quad (2)$$

where y, the vertical run-up, is approximated by the trimline elevation difference. Since frictional energy losses are not accounted for in this calculation, and also given that impact was not perpendicular to flow direction, it provides an estimate of minimum velocity. The lower velocities at point A may reflect underestimation of run-up, as part of the flow appears to have overridden the crest of the valley side here. Our estimates indicate a maximum velocity of ~40 m s^{-1} in the upper El Derrumbe valley, comparable to similar flows elsewhere (e.g. Evans et al. 2001, 2007; Boultbee et al. 2006). Having lost energy in the corner at B, the flow decelerated on the gentler topography of the lower El Derrumbe valley, with extensive deposition of debris, before entering Lago Cabrera.

Lago Cabrera and the 1965 tsunami

Impulse waves in lakes or reservoirs resulting from mass movements have been documented in alpine environments (e.g. Evans 1989; Panizzo et al. 2005) and are a class of tsunami. Field and aerial photograph measurements of wave destruction at Lago Cabrera (Fig. 8) provide a good proxy for tsunami parameters. On steep lakeshore slopes slightly oblique to the direction of wave travel vegetation was completely removed at heights of up to ~30 m above pre-event water level. From this observation, allowing for a small amount of run-up, we estimate that the wave amplitude, η, was ~25 m above ambient water level.

The following calculations rely on lake water depth as an input. We estimate water depth, h, in the centre of the lake by extrapolating topographic slopes (Fig. 8). These suggest that Hornopirén lavas abut early postglacial topography at the base of the Pululil lava ridge, forming a basin that deepens to the east. Active slope sedimentation and debris flow input from the east is likely to have infilled much of this basin in postglacial time, but by an unknown amount. We suggest that the lake depth does not exceed 200 m, but may be as little as 50 m, and use this range in the following calculations.

Wave run-up

The wave run-up in the gently sloping southwest corner of Lago Cabrera provides an additional constraint on wave amplitude and is used to test whether our estimates of wave height are realistic. Here, all buildings and vegetation, except for the largest tree trunks (>1-m diameter), were removed for up to 1,000 m inland, an approximately 50 m climb from the pre-event shoreline. Water travelled beyond this point, but without sufficient energy to remove vegetation, and thus, wave run-up (total vertical height climb of water), R, exceeded 50 m. The minimum ground slope in this region is ~1:20, but the ground steepens towards the shore to ~1:10, and we take this slope as the submerged slope angle, β. We use our estimated wave amplitude, η, of 25 m as a proxy wave source input.

A solitary wave on a planar slope will break when $\eta/h > 0.818\ (\cot\beta)^{-10/9}$ where η/h is the ratio of wave height to water depth (Synolakis 1987). Our lake depth estimates give a η/h range of 0.125–0.5. This exceeds the wave-breaking criterion (0.063 in this case), suggesting that the wave broke early during run-up. Using the numerical results of Li and Raichlen (2002) for plane beach slopes of 1:19.85 and 1:15, R/h is 0.35–0.9, giving an inferred run-up range of 37.5–80 m. This estimate of run-up, which is based on our field-estimated wave height of 25 m, corresponds well with our field observations (R>50 m) and suggests that our estimates are self-consistent and that our lake depth range is plausible.

Wavemaker volume

To estimate the volume of submerged solid material (the wavemaker) that generated the tsunami, we use a model of wave behaviour, constrained by our wave amplitude estimate of η=25 m and using h=100 m (50–200 m range). We work back from this model to find the wavemaker volume, and its dimensions, necessary to produce an impulse wave of this magnitude. Other parameters remain unknown and, consequently, although care is taken to select the most realistic possible assumptions, the volume derived is only approximate.

Following Walder et al. (2003), we divide Lago Cabrera into three regions: the splash zone, extending to the foot of the submerged debris flow and characterised by complex dynamics; the near-field, where kinetic energy is imparted to a coherent wave; and the far-field, where wave propagation effects become significant. The properties of the leading wave

hump in the near-field are, to first order, independent of mass flow type (Walder et al. 2003), with a ratio of amplitude to water depth that is a function of the wavemaker volume and underwater travel time. Walder et al. (2003) provide a scaling analysis where wave properties may be estimated without the need to characterise the complexities of the splash zone. From this, wave amplitude, η, may be expressed as:

$$\eta^* = c\left(\frac{t_s^*}{V_w^*}\right)^{-d} \tag{3}$$

where * indicates a dimensionless variable, t_s is time of submerged debris flow motion, V_w is debris flow volume per unit width (the near-field lake width is 1,000 m) and c and d are regression coefficients of 1.32 and 0.68, respectively. This equation holds true for $2<t_s^*/V_w^*<100$. The dimensionless variables are defined:

$$V_w^* = \frac{V_w}{h^2} \tag{4}$$

$$t_s^* = \frac{[x]}{h'} \tag{5}$$

$$\eta^* = \frac{\eta}{h} \tag{6}$$

where $[x]$ is a distance measure of long-wave water displacement during landslide motion. To estimate V_w^* and η^*, we use a near-field depth (h) in the range of 50–200 m, as discussed above, but to estimate t_s^*, it is necessary to use the depth at the foot of the submerged debris, which we call h'. A first-order approximation for t_s^* is made from (Walder et al. 2003):

$$t_s^* \approx C_s\sqrt{\frac{L}{h'}} \tag{7}$$

where C_s=4.5, appropriate for a Coulomb frictional grain flow (Savage and Hutter 1989), and L is the submerged deposit length, comparable to the extent of the splash zone.

The wavemaker entered the east end of Lago Cabrera in a direction approximately parallel to the lake length and decelerated to rest. We treat the wavemaker as a poorly sorted sedimentary deposit, with an angle of rest (e.g. Carrigy 1970), γ, of 35°. The submerged slope on which the deposit settled is assumed to be formed from previous debris deposits, also with an angle of rest of 35°. The basal lake slope, on which the debris deposits rest, has an unknown angle, θ. The horizontal extent of the submerged fan at the pre-event lake level has been found using the area of the fan at present water level (Fig. 8), assuming a 35° lakeshore slope with a 10-m height change. This area is equivalent to a rectangle with dimensions a (900 m)×b (250 m), and using this, we model the wavemaker as a quadrilateral prism, with centreline length λ (Fig. 8b), such that:

$$V = \lambda ab\sin\gamma \tag{8}$$

where V is the wavemaker volume. From Fig. 8b the values of h' and L are defined as:

$$h' = \sin\gamma\left(\lambda + \frac{\frac{b}{2}\sin\theta}{\sin(\gamma-\theta)}\right) \tag{9}$$

$$L = \sqrt{h'^2 + (b + h'\cot\gamma)^2}. \tag{10}$$

Using Eqs. 3, 4 and 6, 7, 8, 9 and 10, we solve to find λ such that η=25 m, thus producing an estimate of wavemaker volume, V. To achieve this, we relied on our estimates of the poorly constrained parameters γ, θ and h. We tested sensitivity of our results to these input values by varying them within a range of plausible values, with results shown in Table 2. Our assumed submerged deposit angle of rest, γ, of 35° may overestimate the value of a deposit entering the lake with an initial lateral velocity. We find that reducing this value to 20° increases estimated V by 6% (Table 2). Similar sensitivity is shown by changing lake floor slope, θ, within our estimated range of 5–15° (Table 2). Our results are most sensitive to changes in lake depth, h. Within our estimated possible range of 50–200 m, our wavemaker volume varies from 6.5×10^6 to 1.2×10^7. Using what we consider the most likely parameters (Table 2), we estimate a wavemaker volume, V, of ~9±3×10^6 m^3, acknowledging the multiple uncertainties in our calculations, the most significant of which is lake depth. In spite of uncertainties, the ranges of all output parameters fall within a single order of magnitude (Table 2). We estimate that the submerged deposit depth, h', is 55–90 m, with a wavemaker block length, L, of 330–490 m. From this, using Eq. 5, we find a range for $[x]$ of 610–910 m.

Table 2 Tests of the sensitivity of wavemaker and tsunami parameter estimates to input lake parameters

Parameters	Values					
Variables						
γ (°)	35	20	35	35	35	35
θ (°)	10	10	5	15	10	10
h (m)	100	100	100	100	50	200
Results						
h' (m)	68.7	84.4	55.1	90.2	58.4	82.8
L (m)	355	482	329	379	333	368
$[x]$ (m)	703	915	610	843	632	796
V (× 10^6 m^3)	8.8	9.4	9.6	8.1	6.5	12

These results suggest that most of the lake lay within the near-field, which extends to ~3[x] beyond the splash zone, and that wave propagation effects can be neglected.

Our estimates of the wavemaker volume suggest that no more than 50% of the debris flow entered Lago Cabrera. The scale of the tsunami generated is similar to those documented in comparable settings elsewhere, for example the 1946 tsunami at Mount Colonel Foster and Landslide Lake, Canada (η~29 m; R~51 m) which was formed by a smaller wavemaker with volume 7×10^5 m^3 (Evans 1989).

Hydrological effects

Prior to the 1965 landslide, Lago Cabrera's outflow was subterranean and flowed beneath Hornopirén lavas before emerging as the headwaters of the Cuchildeo River, 5 km to the south (Fig. 1). A rapid and sustained increase in water level, estimated at 6 m by eyewitnesses, occurred after the event, indicating disruption of the outflow coupled with water displacement by the submerged deposit. However, the lake level stabilised at an increase of ~10 m. The present-day outflow is observable at the current shoreline in muds adjacent to Hornopirén lavas (Figs. 2 and 4e), and can only have formed here following reestablishment of the lake outflow following the 1965 events.

If the change in lake level was simply due to displacement by the submerged deposit, the wavemaker volume could be directly estimated. For a 10-m change in water level following the event, an original lake area (excluding the 1965 deposit) of 4,438,000 m^2 and a newly flooded area of 918,000 m^2 (Fig. 8c), assuming a linear topographic slope implies a wavemaker volume of ~4.9×10^7 m^3. This volume is considerably larger than that estimated from tsunami modelling ("Wavemaker volume") and greatly exceeds the estimated source area volume in spite of substantial subaerial deposition. Moreover, if used as a starting point in the scaling analysis of Walder et al. (2003), this volume suggests wave amplitude of ~50 m and a resultant run-up (Li and Raichlen 2002) at the SW lake shore of ~90 m, neither of which agree with field observations. We thus infer that hydrological changes in lake outflow took place following the tsunami, with an increase in lake volume of ~4×10^7 m^3, presumably due to riverine input, after equilibration of the lake at a new level. There may also be some seasonal fluctuation in lake volume, which is seen in lake level differences between aerial photographs from 1944 and 1961.

Strike-slip tectonics and edifice stability

Yate lies on the major dextral strike-slip Liquiñe-Ofqui fault zone (Cembrano et al. 1996). Edifice morphology and historic events suggest that major landslides initiate north and south of the volcano summit at an angle of 5–10° to the local trace of the LOFZ towards the Riedel shear direction (Fig. 10). Lagmay et al. (2000) showed how strike-slip fault systems underlying volcanoes may induce edifice instability and produced a structural model of failure for such volcanoes (Fig. 10). Their experiments show that fault shear results in two sigmoids of normal and reverse faults with an internal edifice flower structure, creating two oversteepened and destabilised flank regions where avalanching occurs at angles of 10–20° to the trend of the underlying fault towards the direction of the Riedel shear. We suggest that this model provides a good analogue for the situation at Yate, with the scarps around the north and south failure zones forming sigmoids, exaggerated by subsequent erosion (Fig. 10). This implies that the regional tectonic system is an important factor in determining failure orientation at Yate. There is little historic record of seismic activity on this portion of the LOFZ, though local seismicity indicates dextral strike-slip motion (Lange et al. 2008). The influence of regional tectonics does not imply that large-magnitude fault movement is concurrent with failure, but that instabilities resulting in failure are inherited from movement on the fault over the lifetime of the volcano, concurrent with at least part of the main period of edifice construction. Lagmay et al. (2000) predict that 100 m of motion is sufficient to produce critical instabilities for a cone of 1,500 m in elevation (Yate's summit is ~2,000 m). Although the times and amounts of movement

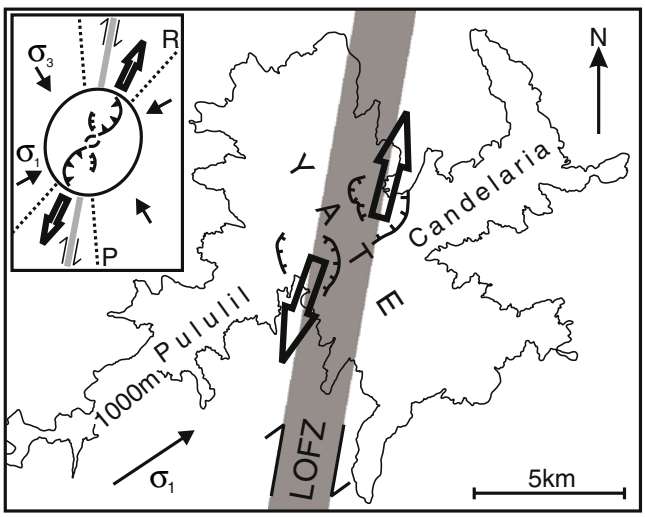

Fig. 10 Map of Yate showing the 1,000-m contour and scars of summit collapses. Directions of failure motion, the line of the LOFZ and the maximum horizontal stress direction for a strike-slip system, σ_1, are shown. The *inset* shows the model results of Lagmay et al. (2000) for edifice failure on a strike-slip fault zone. *P* and *R* show synthetic faults generated in the Lagmay et al. (2000) analogue models, which approximately parallel the P and Riedel shear directions, respectively

on the LOFZ are not well understood, it has been active throughout the Cenozoic (Cembrano et al. 2000; Forsythe and Diemer 2006), and the total Pleistocene–Holocene displacement may fulfil the above failure criterion. However, given the lack of evidence for this order of Holocene movement along this portion of the LOFZ, we speculate that in the case of a glaciated edifice such as Yate, this amount of fault displacement may not be necessary to induce orientated edifice failure.

The first-order role of strike-slip tectonics may be to impose linear zones of weakness within the edifice, forming easily erodible belts that are then exploited by glaciers to initiate orientated glacial valleys. Mechanical weakening, both on the edifice scale by strike-slip faulting and at the surface through glacial action and subsequent debuttressing during deglaciation, may produce a situation with predictable failure directions. The interaction of glaciation with strike-slip tectonics may explain the repetitive but relatively small-scale collapses at Yate, gradually removing masses of mechanically weathered rock, and distinct from the single catastrophic failures at volcanoes such as Iriga, Philippines (Lagmay et al. 2000) where fault movement is greater and the major factor influencing instability. Note also from Fig. 10 that the Candelaria and Pululil ridges radiate away from the main edifice in the direction of maximum horizontal stress (σ_1), suggesting an influence of the regional stress field on the orientation of upper-crustal magma transport (cf. Nakamura 1977) and a further control on volcanism by the regional tectonic regime.

Several other southern Chilean volcanoes also lie along the LOFZ, including stratocones (e.g. Hornopirén), and older complexes, similar to Yate, such as Michinmahuida (Fig. 11). The local tectonic systems at these edifices have implications for hazard assessment in terms of the orientation of mass-wasting events. At Michinmahuida, a large Pleistocene–Holocene composite volcano 115 km south of Yate, a 3-km-wide amphitheatre, interpreted as a caldera, breaches the cone to the north. A similar depression lies south of the summit area from which a large debris-filled valley exits, approximately aligned along the LOFZ. The structure of the edifice is similar to Yate, with N/S-orientated debris-filled valleys on each side of a deeply eroded summit, centred upon a volcanic ridge approximately aligned with the σ_1 direction. These similarities suggest that collapse orientations are influenced by strike-slip tectonics at other volcanoes along the LOFZ. According to Norini and Lagmay (2005), underlying strike-slip fault systems may generate internal stresses and deformation at edifices where the morphology does not suggest such influences. Thus, volcanoes such as Hornopirén, a symmetrical cone elongated along the strike of the LOFZ, may also pose a landslide hazard through specifically orientated slope failure.

Previous landslides at Yate

The two major historic landslides SW of Yate added to an already extensive debris fan in the El Derrumbe valley. Several arcuate scars are evident around the summit of Yate, and the volcano's deeply indented morphology indicates numerous previous collapses of similar style and

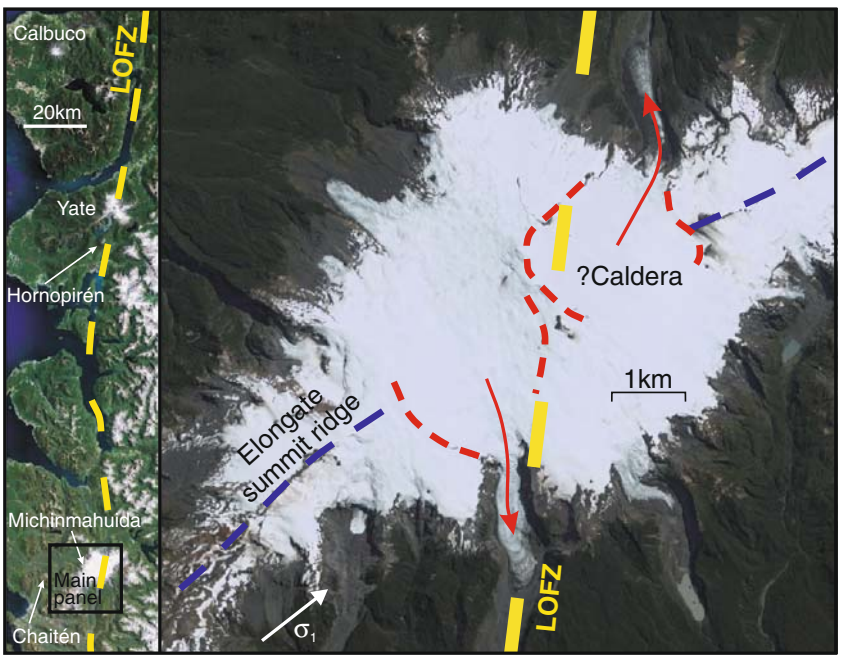

Fig. 11 Aerial image of Michinmahuida volcano. A breached caldera to the north and a depression to the south open at angles slightly oblique to the LOFZ, consistent with the model of Lagmay et al. (2000). The overall structure is similar to Yate, with volcanic ridges parallel to σ_1. The image on the *left* shows the context of these volcanoes on the LOFZ, apparent as a series of fjords and glacial valleys. The location of the main image is *outlined*

magnitude to those of 1965 and 2001. Construction of these deposits has probably occurred throughout postglacial time. Given the present extent of the El Derrumbe fan, only larger debris flows are likely to reach Lago Cabrera and produce tsunamis in the future; most will come to rest on the fan, as in 2001. Prior landslides almost certainly caused tsunamis similar to that of 1965, and the record of these past events should be evident in the sediments of Lago Cabrera. Although the historical records are insufficient to investigate the long-term frequency of landslides, the timing of historic events may provide some insight into the factors controlling failure.

While vegetation was well established in the El Derrumbe valley in 1961, the forest is identifiably less mature on the valley floor than on higher slopes, indicating that events comparable to that of 1965 had occurred within the preceding few hundred years. The 1965 collapse was then followed by another major landslide within less than 40 years. Northeast of the summit, major landslides occurred in 1870 and 1896 from different source regions and with no reported events since. Thus, in spite of the close spacing in time of these historical summit collapses, as compared to the inferred longer term failure rates, it remains unclear whether these failures were structurally related. Historical records, although available over only a short period, suggest a frequency of $\leq 10^2$ years for landslides of 10^6–10^7 m^3 at the summit of Yate.

Although regional tectonics may explain the direction of failure at Yate, the predisposition of the edifice to failure was enhanced by the retreat of ice throughout the Holocene, exposing slopes that were previously stabilised and buttressed by ice. Additionally, incremental eruptive construction of the edifice during the late Pleistocene and early Holocene, for which there is evidence in the summit region, may have generated steeper slopes that became unstable in postglacial time. The lithological composition of the edifice, with massive lavas overlying weaker pyroclastic deposits, may further contribute to instability (Fig. 7; Siebert 1984).

The immediate causes of major landslides include a wide range of external processes, such as extreme rainfall (Iverson 2000), seismicity (Miller 1960; Davis and Karzulovíc 1963; Evans 1989) or a special combination of factors (Kerle et al. 2003), though there may also be no trigger other than the exceedance of a stability threshold. None of the four historic events at Yate correspond to known earthquakes. Hauser (1985) considered that glacial melting associated with high temperatures triggered the 1871 landslide and that extreme rainfall triggered the 1896 event. Unusually heavy rainfall occurred for 15 days prior to the 1965 collapse (eyewitness accounts, Appendix 1), possibly with the 0°C isotherm lying above Yate's summit, and similar weather conditions occurred before the 2001 event. Both events occurred in mid-February, the height of summer, when snow levels are likely to have retreated to their minimum extent, with meltwater increasing pore water pressures. Thus, seasonal temperature effects, coupled with unusually wet weather conditions, may have triggered the past two landslides at Yate. Long periods of intense rainfall, as well as snowmelt, are a well-documented cause of deep-seated, rather than surficial, landslides where the pore water pressure in a body of fractured rock is elevated to failure thresholds (e.g. Schuster and Wieczorek 2002). Yate may have approached critical failure conditions over several decades, perhaps linked to retreating summit ice. Yate is situated within the rupture zone of the May 1960 M_W 9.5 subduction zone earthquake, but in spite of its magnitude, this earthquake did not initiate slope failure. This suggests that in this setting, subduction zone earthquakes, given their distance from the volcanic arc of ~150 km, are a less likely large-landslide trigger than intense summer rainfall, although large earthquakes on the LOFZ (Lange et al. 2008) could provide a seismic triggering mechanism.

In the longer term, hazards of this type may increase on glaciated volcanoes. Glacier retreat between 1961 and 1982 is evident on aerial photographs from those dates (Fig. 3) and has been observed at many southern Andean volcanoes over the past 50 years (Carrasco et al. 2005; Rivera et al. 2005). There is not such a clear change in snowline in aerial photographs from 1944 and 1961, suggesting that glacial retreat may have accelerated at Yate in the latter half of the twentieth century. In addition to seasonal or shorter term changes in pore water pressure due to weather conditions, a longer term increase in meltwater production may destabilise slopes. Furthermore, stress release associated with debuttressing of slopes following ice load removal may condition bedrock for failure (e.g. Cossart et al. 2008) whilst also exposing mechanically weathered rock to further degradation, potentially increasing the likelihood of large landslides. Increased rain rather than snowfall, due to warmer conditions, may further destabilise upper slopes by increased erosion.

Debris flows at Yate appear to have occurred throughout postglacial time, with evidence for multiple events in recent centuries. The factors resulting in recurring collapses at Yate, without magmatic renewal, may be distinct from those that cause significantly larger sector-collapse debris avalanches at many volcanoes. Large Neogene sector-collapse events are well documented at several Central Andean volcanoes (cf. Richards and Villeneuve 2004), with many occurring near the end of the last ice age. An example is that at Parinacota (~6 km^3; Clavero et al. 2002; Hora et al. 2007), which may in part have been induced by rapid deglaciation. At Yate, there is no evidence for events significantly larger than that in 1965. The 1965 landslide volume is over an order of magnitude smaller than many volcanic sector collapses, the largest of which may have a

repeat time of ~1:10 kyr (Ui et al. 2000). However, many volcanoes produce repeated landslides in combination with larger flank failures. For example, Mount Meager, British Columbia, Canada has undergone three flank collapses of $>10^8$ m^3 in the last 7.5 kyr, possibly associated with eruptions (Friele et al. 2005), in addition to numerous smaller landslides, and Mombacho, Nicaragua has displayed similar behaviour (Shea et al. 2008). However, the apparent frequency at Yate of $\leq 10^2$ years for landslides of 10^6–10^7 m^3 is notably high given the lack of volcanism. Landslides of this scale and frequency, originating at the headwalls of erosive features commonly related to structural instabilities, may be common to many volcanoes and may constitute a similar, if not greater, cumulative destructive potential for life and property than that posed by larger landslides or sector collapses. We speculate that Yate's sprawling, glacially eroded composite edifice, its relatively low level of late-Pleistocene and Holocene magmatic activity and its tectonic situation, resulting in deeply incised orientated valleys, may all be contributing factors to such rapid edifice destruction behaviour in discrete landslides of 10^6–10^7 m^3. However, it is possible that the frequency derived from historical records is atypical and that current landslide rates are high, and potentially increasing, due to melting of summit glaciers.

Conclusions

The edifice of Yate has failed in postglacial time through a series of mass movements, generating debris flows that reach the coast to the north and approach Lago Cabrera to the south. The largest historical event occurred in 1965 when a rock face collapsed around a 1.3-km-wide amphitheatre and generated a debris flow. The failed material comprised ice and weathered lavas and pyroclastic rocks. Fifteen days of heavy rain contributed to the failure.

The 1965 debris flow travelled 7,500 m to the shore of Lago Cabrera, descending 1,490 m. Maximum velocity, before deceleration and deposition, is estimated to have been ~40 m s^{-1}. Total deposit volume is estimated at 1.5–2.7×10^7 m^3, at least 50% of which came to rest subaerially. Part of the flow entered the eastern end of Lago Cabrera, producing an impulse wave that caused extensive damage around the lake and killed 27 people living at the southwest shore of the lake. Field evidence and calculations indicate a tsunami wave height of ~25 m with a vertical run-up at the southwest shore of >50 m.

The orientation of landsliding at Yate forms an angle of 10° in the Riedel shear direction to the dextral strike-slip LOFZ on which the volcano is constructed. The orientation corresponds closely to modelled failure directions of volcanoes on strike-slip faults (Lagmay et al. 2000) and is consistent with tectonically mediated collapse. We suggest that movement on the fault within the lifetime of the volcano imposed an orientated weak tectonic fabric, subsequently enhanced by glacial erosion. Additionally, postglacial ice retreat and subsequent erosion may have rendered the upper slopes of thick lavas overlying pyroclastic rocks unstable, promoting mass wasting. Shrinkage of summit glaciers in recent decades, increased meltwater, and greater volumes of rainfall, rather than snow, may have augmented the conditions necessary for failure in 1965 and 2001.

Several southern Chilean volcanoes lie on the LOFZ, and numerous volcanoes globally are situated on strike-slip faults. Many of these volcanoes may be susceptible to edifice collapse in orientations controlled by fault systems. Although volcanic landslide frequency may have increased immediately after late-Pleistocene deglaciation due to processes associated with rapid climatic change (cf. Capra 2006), the hazard from similar events is still present. We cannot estimate long-term rates of edifice collapse, but suggest that melting of summit glaciers and higher altitude rainfall, as a consequence of ongoing climate change, may increase the frequency of large landslides in these environments, particularly on volcanoes where the substrate is mechanically weakened, hydrothermally altered or poorly consolidated. Recognition of deposits from these events and awareness of the hazard to settlements in vulnerable areas are important in mitigating future disasters, particularly when debris flows may interact with water bodies.

Acknowledgements We thank Juan Freddy Antiñirre, Ercilia Mancilla and Antonio Paillén for their personal accounts of events in 1965. We gratefully acknowledge the help of José Luis Urrutia and all CONAF staff at Parque Nacional Hornopirén and Richard Herd for providing the PicWorks photogrammetry application. This work was supported by a NERC studentship to SFLW. TM thanks the Royal Society for funding. We thank John Stix, John Clague and Benjamin van Wyk de Vries for detailed reviews that greatly improved the manuscript.

Appendix 1: Eyewitness accounts

The following is a précis of interviews with eyewitnesses of the 1965 landslide.

Juan Freddy Antiñirre and Ercilia Mancilla (who lost her father, a brother and a sister in the tsunami), Chaihuaco, 15th January 2007: The wave arrived in the early hours of the morning on 19th February 1965, completely destroying three houses at the SW corner of the lake. One house containing two people survived, situated 30 m beyond today's shrine. This land was forested, with mature living coigüe. Twenty-seven lives were lost, and extensive searching, including by boat, yielded only the partial remains of one person. Water, not debris, did the damage,

but ankle-deep soft mud was deposited. The water travelled beyond the region marked by stripped vegetation. At the east lakeshore, there were no signs of previous debris flows; the land was a flat forested valley, farmed, although the one farmhouse there was empty that night. This area was completely buried by rock, snow and ice, leaving hummocks 6–8 m high, and rocks. Following the event, the lake was turbid and contained icebergs and was different in terms of shape and size. The SW shoreline moved by about 100 m and the water level rose by about 6 m. Bubbles appeared occasionally in the shallow water here after the event. Before the event, the Yate summit had a smooth conical profile, resembling a volcano, where the scarp and cliff are today. Unusually bad summer weather, of heavy rainfall, had occurred for 15 days before the landslide.

Antonio Paillén, Hornopirén, 16th January 2007: Corroborated the above account. He was in the house that survived at the SW end of the lake, playing cards at 2.00 A. M. local time, when he heard a noise that he attributes to the rockfall. Water arrived against the walls of his house concurrent with the noise. He lived about 100 m beyond the main zone of damage and noted a second noise after the wave, but only one wave.

References

Branney MJ, Gilbert JS (1995) Ice-melt collapse pits in the 1991 lahar deposits of Volcán Hudson, Chile: criteria to distinguish eruption-induced glacier melt. Bull Volcanol 57:293–302

Boultbee N, Stead D, Schwab J, Geertsema M (2006) The Zymoetz River rock avalanche, June 2002, British Columbia, Canada. Eng Geol 83:76–93

Capra L (2006) Abrupt climatic changes as triggering mechanisms of massive volcanic collapses. J Volcanol Geotherm Res 155:329–333

Carrasco JF, Casassa G, Quintana J (2005) Changes of the 0°C isotherm and the equilibrium line altitude in central Chile during the last quarter of the 20th century. Hydrol Sci J 50:933–948

Carrigy MA (1970) Experiments on the angles of repose of granular materials. Sedimentology 14:147–158

Cembrano J, Hervé F, Lavenu A (1996) The Liquiñe Ofqui fault zone: a long-lived intra-arc fault system in southern Chile. Tectonophysics 59:5–66

Cembrano J, Schermer E, Lavenu A, Sanhueza A (2000) Contrasting nature of deformation along an intra-arc shear zone, the Liquiñe-Ofqui fault zone, southern Chilean Andes. Tectonophysics 319:129–149

Clavero J, Sparks RSJ, Huppert HE, Dade WB (2002) Geological constraints on the emplacement mechanism of the Parinacota debris avalanche, northern Chile. Bull Volcanol 64:40–54

Cossart E, Braucher R, Fort M, Bourlès DL, Carcaillet J (2008) Slope instability in relation to glacial debuttressing in alpine areas (Upper Durance catchment, southeastern France): evidence from field data and ^{10}Be cosmic ray exposure ages. Geomorphology 95:3–26

CONAF (2007) Parque Nacional Hornopirén, chapter 2: Recursos y características naturales y culturales. CONAF (Corporación Nacional Forestal, Chile) internal document

Davis SN, Karzulovíc JK (1963) Landslides at Lago Riñihue, Chile. Bull Seismol Soc Am 53:1403–1414

El Mercurio (2001) Aluvión en Cochamó. El Mercurio, Santiago, Chile, 15th February 2001

Evans SG (1989) The 1946 Mount Colonel Foster rock avalanche and associated displacement wave, Vancouver Island, British Columbia. Can Geotech J 26:447–452

Evans SG, Clague JJ, Woodsworth GJ, Hungr O (1989) The Pandemonium Creek rock avalanche, British Columbia. Can Geotech J 26:427–446

Evans SG, Hungr O, Clague JJ (2001) Dynamics of the 1984 rock avalanche and associated distal debris flow on Mount Cayley, British Columbia, Canada; implications for landslide hazard assessment on dissected volcanoes. Eng Geol 61:29–51

Evans SG, Guthrie RH, Roberts NJ, Bishop NF (2007) The disastrous February 17, 2006 rockslide–debris avalanche on Leyte Island, Philippines: a catastrophic landslide in tropical mountain terrain. Nat Haz Earth Syst Sci 7:89–101

Flash (1965) El lago Cabrera ahogo a un pueblo. Flash, Santiago, Chile, 26th February 1965, no. 84, Año 11, aero norte

Forsythe RD, Diemer JA (2006) Late Cenozoic movement associated with the arc-parallel Liquiñe-Ofqui fault zone and the Chile triple junction documented by acoustic profiling of shallow marine and lacustrine deposits of southern Chile. Geol Soc Am Abstracts with Programs, Speciality Meeting No. 2 (Backbone of the Americas–Patagonia to Alaska), 48

Friele PA, Clague JJ, Simpson K, Stasiuk M (2005) Impact of a Quaternary volcano on Holocene sedimentation in Lillooet River valley, British Columbia. Sediment Geol 176:305–322

Hauser AY (1985) Flujos aluvionales de 1870 y 1896 ocurridos en la ladera norte del volcan Yates, X región: su implicancia en la evolución de riesgos naturales. Rev Geol Chile 25–26:125–133

Heusser CJ (2002) On glaciation of the southern Andes with special reference to the Península de Taitao and adjacent Andean cordillera (~46°30′S). J S Am Earth Sci 15:577–589

Hora JM, Singer BS, Wörner G (2007) Volcano evolution and eruptive flux on the thick crust of the Andean Central Volcanic Zone: ^{40}Ar/^{39}Ar constraints from Volcán Parinacota, Chile. Geol Soc Amer Bull 119:343–362

Huggel C, Caplan-Auerbach J, Waythomas JCF, Wessels RL (2007) Monitoring and modeling ice–rock avalanches from ice-capped volcanoes: a case study of frequent large avalanches on Iliamna Volcano, Alaska. J Volcanol Geotherm Res 168:114–136

Hungr O, Evans SG (2004) Entrainment of debris in rock avalanches: an analysis of a long run-out mechanism. Geol Soc Amer Bull 116:1240–1252

Iverson RM (2000) Landslide triggering by rain infiltration. Water Resour Res 36:1897–1910

Jakob M (2005) A size classification for debris flows. Eng Geol 79:151–161

Kerle N (2002) Volume estimation of the 1998 flank collapse at Casita volcano, Nicaragua—a comparison of photogrammetric and conventional techniques. Earth Surf Processes Landforms 27:759–772

Kerle N, van Wyk de Vries B, Oppenheimer C (2003) New insights into the factors leading to the 1998 flank collapse and lahar disaster at Casita volcano, Nicaragua. Bull Volcanol 65:331–345

Lagmay AMF, van Wyk de Vries B, Kerle NA, Pyle DM (2000) Volcano instability induced by strike-slip faulting. Bull Volcanol 62:331–346

Lange D, Cembrano J, Rietbrock A, Haberland C, Dahm T, Bataille K (2008) First seismic record for intra-arc strike-slip tectonics along the Liquiñe-Ofqui fault zone at the obliquely convergent plate margin of the southern Andes. Tectonophysics 455:14–24

Li Y, Raichlen F (2002) Non-breaking and breaking solitary wave run-up. J Fluid Mech 456:295–318

Miller DJ (1960) Giant waves in Lituya Bay Alaska. US Geol Surv Prof Pap 354-C:1–86

Nakamura K (1977) Volcanoes as possible indicators of tectonic stress orientation—principle and proposal. J Volcanol Geotherm Res 2:1–16

Norini G, Lagmay AMF (2005) Deformed symmetrical volcanoes. Geology 33:605–608

Panizzo A, De Girolamo P, Di Risio M, Maistri A, Petaccia A (2005) Great landslide events in Italian artificial reservoirs. Nat Haz Earth Syst Sci 5:733–740

Pierson TC (1985) Initiation and flow behaviour of the 1980 Pine Creek and Muddy River lahars, Mount St. Helens, Washington. Geol Soc Amer Bull 96:1056–1069

Richards JP, Villeneuve M (2004) The Llullaillaco Volcano, northwest Argentina: construction by Pleistocene volcanism and destruction by sector collapse. J Volcanol Geotherm Res 132:337–365

Rivera A, Bown F, Casassa G, Acuña C, Clavero J (2005) Glacier shrinkage and negative mass balance in the Chilean Lake District (40°S). Hydrol Sci J 50:963–974

Savage SB, Hutter K (1989) The motion of a finite mass of granular material down a rough incline. J Fluid Mech 199:177–215

Schuster RL, Wieczorek GF (2002) Landslide triggers and types. In: Rybář J, Stemberk J, Wagner P (eds) Landslides. Proceedings of the 1st European Conference on Landslides. Prague, June 24–26, pp 59–78

Scott K, Macías JL, Naranjo JA, Rodríguez S, McGeehin JP (2001) Catastrophic debris flows transformed from landslides in volcanic terrains: mobility, hazard assessment, and mitigation strategies. US Geol Surv Prof Pap 1630:1–59

Scott KM, Vallance JW, Kerle N, Macías JL, Strauch W, Devóli G (2005) Catastrophic precipitation-triggered lahar at Casita volcano, Nicaragua: occurrence, bulking and transformation. Earth Surf Processes Landforms 30:59–79

Sepúlveda SA, Rebolledo S, Vargas G (2006) Recent catastrophic debris flows in Chile: geological hazard, climatic relationships and human response. Quat Int 158:83–95

Shea T, van Wyk de Vries B, Pilato M (2008) Emplacement mechanisms of contrasting debris avalanches at Volcán Mombacho (Nicaragua), provided by structural and facies analysis. Bull Volcanol 70:899–921

Siebert L (1984) Large volcanic debris avalanches: characteristics of source areas, deposits, and associated eruptions. J Volcanol Geotherm Res 22:163–197

Synolakis CE (1987) The runup of solitary waves. J Fluid Mech 185:523–545

Ui T, Takarada S, Yoshimoto M (2000) Debris avalanches. In: Sigurdsson H, Houghton B, McNutt S, Rymer H, Stix J (eds) Encyclopedia of volcanoes. Academic, San Diego, pp 617–626

Walder JS, Watts P, Sorensen OE, Janssen K (2003) Tsunamis generated by subaerial mass flows. J Geophys Res 108:B5, 2236